

Diffractive Production of ρ Mesons by 147-GeV Muons*

W. R. Francis, H. L. Anderson, V. K. Bharadwaj, N. E. Booth, R. M. Fine,[†] B. A. Gordon,
R. H. Heisterberg,[‡] R. G. Hicks, T. B. W. Kirk, G. I. Kirkbride,[§] W. A. Loomis,
H. S. Matis, L. W. Mo,[‡] L. C. Myriantopoulos, F. M. Pipkin, S. H. Pordes,^{||}
T. W. Quirk, W. D. Shambroom, A. Skuja,[¶] L. J. Verhey,^{**}
W. S. C. Williams, Richard Wilson, and S. C. Wright

*Enrico Fermi Institute and Department of Physics, The University of Chicago, Chicago, Illinois 60637, and
Department of Physics, Harvard University, Cambridge, Massachusetts 02138, and Department of
Physics, The University of Illinois at Urbana-Champaign, Urbana, Illinois 61801, and Nuclear
Physics Laboratory, The University of Oxford, Oxford, OX1 3RH, England*

(Received 21 December 1976)

Cross sections for diffractive ρ muoproduction in hydrogen are presented for $90 \text{ GeV} < \nu < 135 \text{ GeV}$ (where ν is the energy lost by the scattered muon) and $Q^2 < 5 \text{ (GeV}/c)^2$. The results are compared with lower-energy data and the predictions of simple vector-dominance models.

We have extended the study of ρ -meson lepto-production to higher energies. The experiment was performed at the Fermi National Accelerator Laboratory as part of a comprehensive program of muon scattering using the spectrometer constructed by this group.

Details of the apparatus have been described in previous Letters.¹ Positive muons of 147 GeV were incident upon a 1.19-m liquid-hydrogen target. The experiment trigger required that a muon leave the beam by scattering through a large angle ($\gtrsim 14 \text{ mrad}$) or by suffering a large energy loss ($\gtrsim 85 \text{ GeV}$), or both. In this paper, data are reported for which $90 \text{ GeV} < \nu < 135 \text{ GeV}$ and $Q_{\text{min}}^2 < Q^2 < 5.0 \text{ (GeV}/c)^2$, where ν is the energy lost by the scattered muon, Q^2 is the square of the muon four-momentum transfer, and Q_{min}^2 is the minimum kinematically allowed value of Q^2 at a given ν .

The 2.17×10^{10} incident muons yielded 150K triggers. Events in which a scattered muon was reconstructed were examined for evidence of the production of hadronic pairs. The selection criteria required that one positive and one negative particle be observed in addition to the scattered

muon, that the production vertex occur within the target volume, and that the measured secondary energies reconstruct the energy of the incident muon within 3.0 GeV ($\sigma_{\text{RMS}} = 1.1 \text{ GeV}$).

The invariant mass of these neutral pairs was calculated by assuming that both particles were pions. This sample contained a large number ($\sim 70\%$) of low-mass ($< 0.5 \text{ GeV}$), electron-positron pairs from purely electromagnetic processes. These were identified by observing their cascade showers behind a 3-radiation-length steel radiator. Since pions could also generate

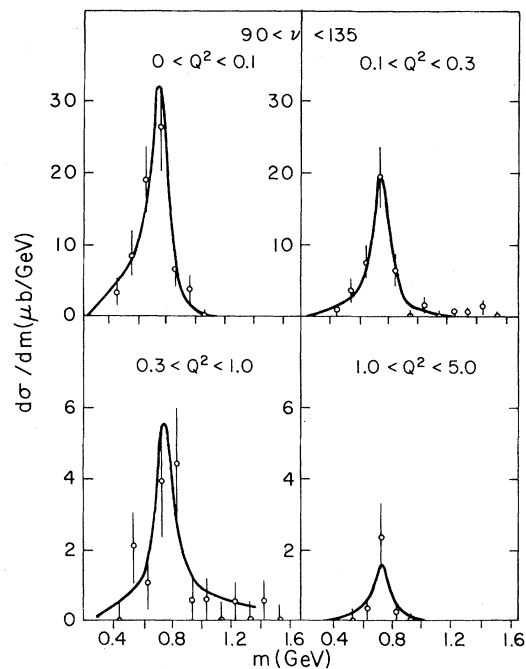


FIG. 1. Dipion mass spectra for various Q^2 ranges.

TABLE I. Bin kinematics.

Q^2 (GeV^2/c^2)	$\langle Q^2 \rangle$ (GeV^2/c^2)	$\langle \nu \rangle$ (GeV)	$\langle \epsilon \rangle$	Events
0.01–0.10	0.04	102	0.56	41
0.02–0.10	0.06	118	0.40	33
0.1–0.3	0.16	104	0.55	27
0.1–0.3	0.18	124	0.33	43
0.3–1.0	0.62	115	0.41	29
1.0–5.0	2.2	106	0.51	11

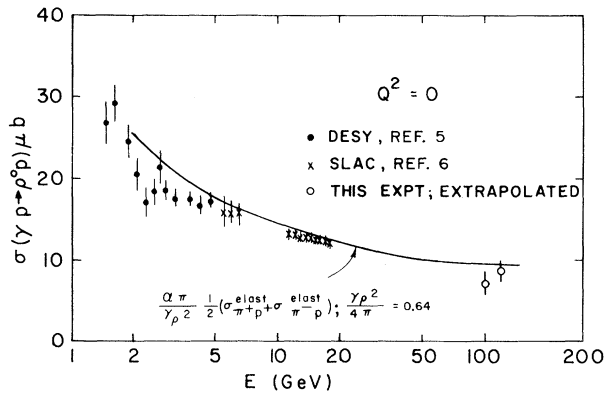


FIG. 2. Diffractive ρ photoproduction cross sections.

such showers, a clean separation of events was achieved by demanding a pair opening angle greater than 5.0 mrad ($\sigma_{\text{RMS}} = 0.6$ mrad).

Polynomial fits to the background outside the energy-balance cut indicated a 16% contamination due to hadronic pairs with one or more undetected, slow pions. This background was reduced to $(3 \pm 2)\%$, approximately independent of Q^2 and ν , by requiring that t , the square of the four-momentum transfer to the proton, satisfy $t < 0.8$ $(\text{GeV}/c)^2$ ($\sigma_{\text{RMS}} \sim \frac{1}{8}\sqrt{t}$ GeV/c).

The resulting sample of hadron pairs contained 184 events. These data were grouped into bins of Q^2 and ν (Table I), and corrected for beam-reconstruction losses (24%), pion absorption (6.5% per pion), chamber inefficiencies (7.0% per particle), reconstruction inefficiencies for tracks close to the beam (between 0 and 46%; 5% on the average), trigger inefficiencies (between 2 and 12%; average, 7%), multiple scattering and resolution smearing (between 1 and 8%; average, 3%), and geometric acceptance. The liquid hydrogen

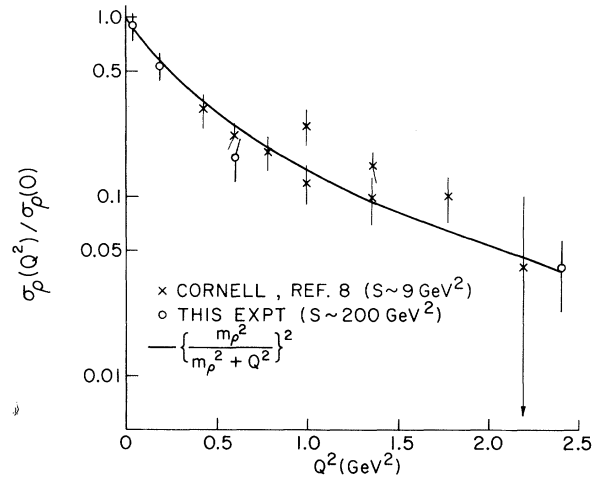


FIG. 3. Q^2 dependence of diffractive ρ muoproduction.

constituted 95% of the target mass. Since insufficient empty-target dipion data were available for a simple subtraction, a 5% correction factor was employed to remove the contribution from the target vessel. The total systematic uncertainty is estimated at 7%.

Dividing by the usual virtual-photon flux factor,² we derive cross sections $d\sigma(Q^2, \nu, \epsilon, m, t) / dm dt$ for the reaction $\gamma_{\text{virtual}} + p \rightarrow \pi^+ + \pi^- + p$. Here m is the dipion mass; ϵ , the virtual-photon polarization parameter. Radiative corrections were applied following the general formalism of Bartl and Urban.³ These increased the observed cross section by an average of 3% at $Q^2 = 0.05$; 8%, at $Q^2 = 2.5$ $(\text{GeV}/c)^2$. In each Q^2 - ν bin the cross section was integrated over t . Following the prescription of Spital and Yennie,⁴ the spectra were fitted in the mass interval 0.4 to 1.1 GeV to the following form, smeared by the calculated resolution so that

$$\frac{d\sigma}{dm} = \frac{C_1 m m_\rho \Gamma}{(m_\rho^2 - m^2)^2 + m_\rho^2 \Gamma^2} \left[1 + C_2 \left(\frac{m_\rho^2 - m^2}{m^2} \right) + C_3 \left(\frac{m_\rho^2 - m^2}{m^2} \right)^2 \right],$$

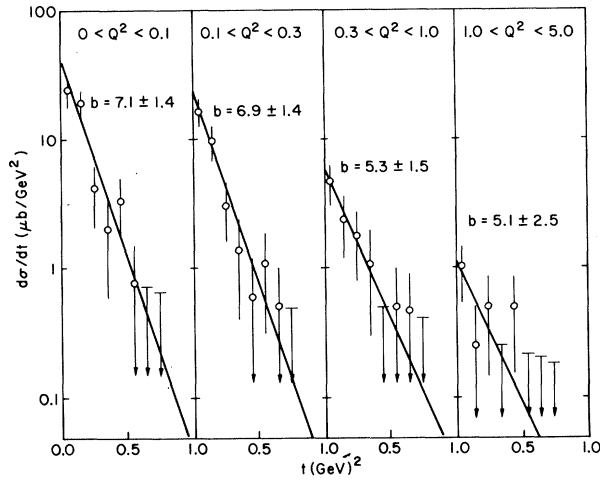
where

$$\Gamma = \Gamma_\rho \frac{m_\rho}{m} \left(\frac{m^2 - 4m_\pi^2}{m_\rho^2 - 4m_\pi^2} \right)^{3/2},$$

and the C 's are the free parameters of the fit. The ρ mass and width were fixed throughout at 0.77 and 0.15 GeV, respectively. The results of the fits were used to obtain cross sections $\sigma_\rho(Q^2)$, for the process $\gamma_{\text{virtual}} + p \rightarrow \rho + p$. Figure 1 presents the unsmeared mass spectra and fits.

Photoproduction cross sections were extrapolated from the measurements below $Q^2 = 0.3$ $(\text{GeV}/c)^2$ assuming $\sigma_\rho(Q^2) = \sigma_\rho(0)(1 + Q^2/m_\rho^2)^{-2}$.

Figure 2 compares these results with representative lower-energy data.^{5,6} The curve is the quark-model prediction relating this process to elastic pion scattering via the vector-dominance model

FIG. 4. t dependence of dipions with $0.6 < m_{\pi\pi} < 1.0$.

(VDM)⁷ calculated using the colliding-beam value for the ρ -photon coupling constant. Although the data exhibit no significant energy dependence within our kinematic range, the real photoproduction cross section falls from about $20 \mu\text{b}$ at $s = 5 \text{ GeV}^2$ to $7.9 \pm 0.8 \mu\text{b}$ near $s = 200 \text{ GeV}^2$. The observed decrease agrees well in both shape and magnitude with this model.

Figure 3 displays the Q^2 dependence of the observed production cross section, averaged over ν , along with low-energy data from Ahrens *et al.*⁸ Once the s dependence of the real photon cross section is removed, the data are remarkably energy-independent and fit quite well the same ρ -propagator-squared form factor used in the photoproduction extrapolation. Considering the difference between virtual-photon beam polarizations in the two experiments, agreement at this

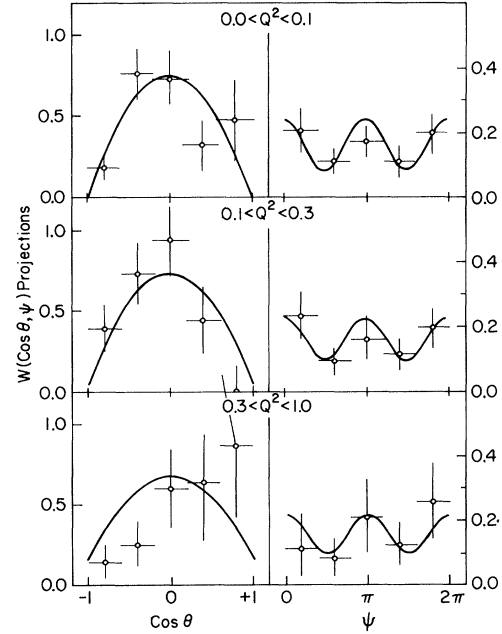


FIG. 5. Decay angular distributions.

level is not predicted by the simple VDM.⁹

Pairs with mass between 0.6 and 1.0 GeV were analyzed in further detail. The t distributions were fitted to a simple exponential, $A \exp(-bt)$. Figure 4 displays these data and fits for various Q^2 bins. The data suggest a broadening with increasing Q^2 but are also consistent with a single slope parameter $b = 6.4 \pm 0.8 (\text{GeV}/c)^{-2}$.

The angular distribution of the decay pions has been studied, yielding information on the spin structure of the production process. The assumption of s -channel helicity conservation (SCHC) and dominance of natural-parity exchange¹⁰ predicts the decay distribution

$$W(\cos\theta, \psi) = \frac{1}{1 + \epsilon R_\rho} \frac{3}{8\pi} \left\{ \sin^2\theta (1 + \epsilon \cos 2\psi) + 2\epsilon R_\rho \cos^2\theta \right. \\ \left. - [2\epsilon(1 + \epsilon)R_\rho]^{1/2} \cos\delta \sin 2\theta \cos\psi + [2\epsilon(1 - \epsilon)R_\rho]^{1/2} P \sin\delta \sin 2\theta \sin\psi \right\},$$

where R_ρ is the ratio of the longitudinal to the transverse ρ production cross section, δ is the phase difference between the longitudinal and the transverse amplitudes, and P is the average muon-beam polarization (~ 0.8). Here θ is the polar angle of the π^+ in the ρ rest frame with z axis opposite to the direction of the recoil proton, and ψ is the azimuthal angle of the π^+ referenced to the muon scattering plane. The values of R and δ were varied to give the best fit to the data.

Figure 5 displays the data and fits for several Q^2 bins. The results of the fits are presented in

TABLE II. SCHC fit results.

$\langle Q^2 \rangle$ (GeV^2/c^2)	$\langle \epsilon \rangle$	R_ρ	δ (deg)
0.05	0.49	$0.00^{+0.04}_{-0}$	Indeterminate
0.17	0.41	$0.05^{+0.08}_{-0.05}$	-6 ± 37
0.62	0.41	$0.3^{+0.4}_{-0.2}$	5 ± 38
2.2	0.51	$0.5^{+0.6}_{-0.4}$	-60 ± 33

Table II. The parameters of high-energy production are a smooth continuation of the trends of the low-energy data¹¹ with R_ρ now remaining small as Q^2 increases to 2.2 (GeV/c)². The phase difference is consistent with zero except, perhaps, in the highest Q^2 bin.

We thank the staffs of Fermilab, of our home institutions, and of the Rutherford Laboratory whose help made this work possible. We gratefully acknowledge numerous discussions with and suggestions by Dr. Garland Grammer on the subject of radiative corrections.

*Work supported by the National Science Foundation under Contract No. MPS 71-03-186, by the U. S. Energy Research and Development Administration under Contract Nos. E(11-1)-3064 and No. 1195, and by the Science Research Council (United Kingdom).

†Present address: Nevis Laboratory, Columbia University, New York, N. Y. 10027.

‡Present address: Physics Department, Virginia Polytechnic Institute and State University, Blacksburg, Va. 24061.

§Present address: Hanson Laboratory, Stanford Laboratory, Stanford University, Stanford, Calif. 94305.

¶Present address: CERN, Geneva, Switzerland.

‡Present address: Physics Department, University of Maryland, College Park, Md. 20742.

**Present address: Massachusetts General Hospital, Boston, Mass. 02125.

¹W. A. Loomis *et al.*, Phys. Rev. Lett. 35, 1483 (1975); H. L. Anderson *et al.*, Phys. Rev. Lett. 37, 4 (1976).

²L. N. Hand, Phys. Rev. 129, 1834 (1964).

³A. Bartl and P. Urban, Acta Phys. Austriaca 24, 139 (1966).

⁴R. Spital and D. R. Yennie, Phys. Rev. D 9, 126 (1974).

⁵Aachen-Berlin-Bonn-Hamburg-Heidelberg-München Collaboration, Phys. Rev. 175, 1669 (1968).

⁶R. Anderson *et al.*, Phys. Rev. D 1, 27 (1970).

⁷H. Joos, Phys. Lett. 24B, 103 (1967).

⁸L. Ahrens *et al.*, Phys. Rev. Lett. 31, 131 (1973), and Phys. Rev. D 9, 1894 (1974).

⁹H. Fraas and D. Schildknecht, Nucl. Phys. B14, 543 (1969); C. F. Cho and G. J. Gounaris, Phys. Rev. 186, 1619 (1969).

¹⁰K. Schilling and G. Wolf, Nucl. Phys. B61, 381 (1973).

¹¹P. Joos *et al.*, Nucl. Phys. B113, 53 (1976).

Relativistic Two-Body Wave Equation and Meson Spectrum

H. Suura*

School of Physics and Astronomy, University of Minnesota, Minneapolis, Minnesota 55455

(Received 19 October 1976)

The meson spectrum is studied with use of an equal-time relativistic two-body equation with electrostatic confinement potentials. A normalizability condition excludes all but a bag solution which gives a spectral pattern in between the SU(6) and the chiral SU(3) × SU(3) limits. Orbital mixing creates a pair of ³S₁ + ³D₁ states sandwiching the ¹P₁ level. ρ - ρ' and ψ / J - ψ' pairs fit this picture very well.

Fully relativistic studies of quark-antiquark systems have been done in the past using the Bethe-Salpeter equation, as in the extensive works by Böhm, Krammer, and Joos,¹ which were based on the concept of the effective quark confinement due to large quark masses. The concept may still prove to be a viable one, but in the alternative color confinement scheme the conventional definition of the Bethe-Salpeter amplitude would fail. This is because infinitely high frequencies of the colored intermediate states force such an amplitude to vanish. Therefore, I propose to investigate instead a relativistic two-body wave equation of the form

$$\begin{aligned} (-i\alpha \cdot \nabla + \beta m_1)\chi(\vec{r}) - \chi(\vec{r})(-i\alpha \cdot \nabla + \beta m_2) \\ = [M - V(r)]\chi(\vec{r}). \end{aligned} \quad (1)$$

Here the wave function χ is given a 4×4 matrix representation $\chi_{\alpha\beta}$, with indices α and β referring to quark and antiquark spinor components, respectively. I have taken the center-of-mass system and \vec{r} is a relative coordinate. m_1 and m_2 are the quark masses and M is the eigenvalue of the system. The potential $V(r)$, which I assume to be electric in origin as indicated by some confinement models,^{2,3} appears in the combination $M - V$, rather than in the combination of $m_{1,2} - V$ for Lorentz-scalar potentials. The equation differs from the Breit equation,⁴ based on the one-quantum-exchange approximation, in lacking the current-current interaction term. However, relativistic covariance does not necessarily require the presence of such a term, as can be seen from the following example of a covariant generaliza-